

# Comparative Study of Anti-hepatitis B Virus RNA Interference by Double-stranded Adeno-associated Virus Serotypes 7, 8, and 9

Chun-Chi Chen<sup>1,2</sup>, Cheng-Pu Sun<sup>2,3</sup>, Hsin-I Ma<sup>4</sup>, Cheng-Chieh Fang<sup>2</sup>, Pin-Yi Wu<sup>2</sup>, Xiao Xiao<sup>5</sup> and Mi-Hua Tao<sup>2</sup>

<sup>1</sup>Graduate Institute of Microbiology, National Taiwan University, Taipei, Taiwan; <sup>2</sup>Institute of Biomedical Sciences, Academia Sinica, Taipei, Taiwan; <sup>3</sup>Taiwan International Graduate Program, Academia Sinica and National Yang-Ming University, Taipei, Taiwan; <sup>4</sup>Department of Neurological Surgery, Tri-Service General Hospital, and the National Defense Medical Center, Taipei, Taiwan; <sup>5</sup>Department of Pathology, University of North Carolina School of Medicine, Chapel Hill, North Carolina, USA

Using a hepatitis B virus (HBV) transgenic mouse model, we previously showed that a single dose of double-stranded adeno-associated virus (dsAAV) vector serotype 8 carrying a small hairpin RNA (shRNA) effectively reduces HBV replication and gene expression, but the effect gradually decreases with time. In this report, we compared the anti-HBV RNA interference (RNAi) effect of dsAAV8 with those of dsAAV7 and dsAAV9, two other hepatotropic AAV vectors, and examined whether the sequential use of these heterologous AAV vectors could prolong the anti-HBV effect. Our results showed that shRNA delivered by each of the three dsAAV vectors profoundly reduced the serum HBV titer and liver HBV mRNA and DNA levels in the transgenic mice for up to 22 weeks, with dsAAV8 having the greatest inhibitory effect, followed by dsAAV9 and dsAAV7. The potency of dsAAV8 correlated with the presence of higher levels of vector DNA and anti-HBV shRNA in the liver. An *in vivo* cross-administration experiment showed that preexisting anti-AAV8 antibody completely blocked the anti-HBV RNAi effect of dsAAV8, but had no effect on the potency of dsAAV7 and dsAAV9. Moreover, we demonstrated that a longer anti-HBV effect could be achieved by the sequential use of dsAAV8 and dsAAV9. These results indicate that effective and persistent HBV suppression might be achieved by a combination of the power of RNAi silencing effect and multiple treatments with different AAV serotypes.

Received 11 June 2008; accepted 6 October 2008; published online 9 December 2008. doi:10.1038/mt.2008.245

## INTRODUCTION

Hepatitis B virus (HBV) infection remains a serious infectious disease, resulting in ~350 million chronically infected patients worldwide. Patients chronically infected with HBV suffer from liver complications, including cirrhosis and hepatocellular carcinoma, leading to >1 million deaths every year.<sup>1,2</sup> Recent reports

have revealed that the incidence of hepatocellular carcinoma in chronic HBV patients is positively correlated with HBV titer and HBeAg expression level.<sup>3,4</sup> Accordingly, the final goal for chronic HBV therapy is to achieve long-term HBV suppression, thus preventing the progression of liver diseases. Current anti-HBV therapies include immunomodulators, such as interferon- $\alpha$ -2a and PEGylated interferon- $\alpha$ -2b, as well as nucleoside and nucleotide analogs, such as lamivudine, adefovir dipivoxil, entecavir, which inhibit HBV reverse transcriptase and thus viral replication.<sup>5</sup> However, these anti-HBV drugs have limited effectiveness in completely eliminating the virus, leading to selection of drug-resistant mutations and a high rate of relapse when treatment is discontinued.<sup>6</sup> Thus, the development of new treatment strategies for chronic HBV remains a major medical challenge.

RNA interference (RNAi) is an evolutionary conserved mechanism in which gene expression is inhibited through mRNA degradation using small RNA fragments with completely complementary sequences to the mRNA being degraded. There are ample reports demonstrating that RNAi has great potential as a new therapeutic agent for infectious diseases.<sup>7-9</sup> In terms of HBV infection, early *in vitro* studies provided proof-of-principle that synthetic small interfering RNA (siRNA) or plasmid-encoded small hairpin RNA (shRNA) can effectively repress viral replication and gene expression.<sup>10-13</sup> The *in vivo* anti-HBV effect of RNAi was initially evaluated in animal models established by hydrodynamic co-injection of HBV expression plasmids and anti-HBV siRNA or shRNA expression plasmids.<sup>11,14</sup> Moreover, the *in vivo* anti-HBV effect can be enhanced by chemical modification and lipid-encapsulation of siRNAs.<sup>15,16</sup> However, because of the transient nature of the suppression and the inefficient delivery of these approaches, synthetic siRNAs and plasmid-encoded shRNAs are unlikely to have durable anti-HBV effects in more stringent HBV infection conditions, such as in HBV transgenic mice or in chronically infected HBV patients, as virtually all hepatocytes are infected in these subjects. In this regard, the use of a shRNA-expressing viral vector, which can achieve efficient and uniform transduction of all liver cells to produce a more sustained RNAi effect, represents an attractive approach to the treatment of chronic HBV infection.

The first two authors contributed equally to this work.

Correspondence: Mi-Hua Tao, 128 Academia Road, Section 2, Institute of Biomedical Sciences, Academia Sinica, Taipei 11529, Taiwan. E-mail: bmtao@ibms.sinica.edu.tw

Adeno-associated virus (AAV), with an excellent safety profile and effectiveness of *in vivo* transgene expression, has gained popularity in gene therapy applications over the past decade.<sup>17,18</sup> Several preclinical studies have revealed that AAV serotype 8 is particularly efficient in transducing the liver.<sup>19–22</sup> In our previous study,<sup>23</sup> we developed several shRNA-expressing double-stranded AAV2/8 vectors (dsAAV8) to deliver anti-HBV shRNAs and evaluated their therapeutic efficacy in a HBV transgenic mouse model, which produces up to  $1 \times 10^9$  viral genomes in the circulation, comparable to that found in chronic HBV patients. We showed that a single injection of the dsAAV8 vector, carrying one particular HBV-specific shRNA, had a potent suppressive effect that almost completely depleted HBV replication in the liver, leading to an up to  $3 \log_{10}$  decrease in HBV load in the circulation, and that this inhibitory effect lasted for up to 4 months without apparent toxicity. Nevertheless, the RNAi-mediated HBV suppressive effect slowly decreased with time, accompanied by a gradual loss of the AAV genome in the mouse liver.

In this study, we compared the anti-HBV RNAi effect of dsAAV8 with those of two recently isolated AAV serotypes, dsAAV7 and dsAAV9, which also show high liver transduction efficiency.<sup>19,24</sup> We also examined whether repeated injections of different AAV serotypes carrying shRNA could extend the duration of the anti-HBV effect. The multiple treatment strategy was designed based on several previous reports that repeated administration of immunologically distinct AAV serotypes can successfully prolong transgene expression and increase its levels.<sup>25–27</sup>

## RESULTS

### Comparison of liver transduction efficiency of dsAAV7, dsAAV8, and dsAAV9

On the basis of previous reports, which demonstrated a remarkable tropism of AAV7, AAV8, and AAV9 for the liver,<sup>19,24</sup> we chose these three dsAAV serotypes to deliver shRNA for HBV treatment. For a direct comparison of these vectors in liver gene delivery, we prepared AAV vectors containing an identical AAV2-based DNA cassette containing the *green fluorescent protein (GFP)* gene driven by a constitutive CMV enhancer/ $\beta$ -actin (CB) promoter. Since the AAV2 genome was designed to include a deletion in the terminal resolution site in one end of the inverted terminal repeat, the final AAV vectors contained double-stranded genomes. These vectors were designated as dsAAV7/CB-GFP, dsAAV8/CB-GFP, and dsAAV9/CB-GFP. Wild-type ICR mice were intravenously (IV) injected with  $1 \times 10^{12}$  vector genomes (vg) per mouse of one of the vectors and killed 3 weeks later to analyze GFP expression in the liver by fluorescence microscopy. As shown in **Figure 1a**, injection with each of the three dsAAV serotypes resulted in high GFP expression in the mouse liver. Interestingly, dsAAV8 and dsAAV9 gave a relatively uniform GFP distribution in the liver, whereas dsAAV7 transduction was essentially confined to the centrilobular region. Quantification of the fluorescence intensity revealed that the dsAAV8 vector gave the highest level of GFP expression, resulting in 3.6- or 6.6-fold greater fluorescence intensity than that obtained with the dsAAV9 or dsAAV7 vector, respectively (**Figure 1b**, upper panel). Calculation of the percentage of the total area that contained GFP-positive cells showed a similar pattern of transduction ability of these three dsAAV vectors, with ~65% of

hepatocytes being infected by dsAAV8, significantly higher than the 50 and 34% transduction rate achieved using dsAAV9 and dsAAV7, respectively (**Figure 1b**, lower panel). These results demonstrate that, of the three liver-tropic vectors examined, dsAAV8 was the most efficient in directing liver gene transfer.

### Comparison of the efficacy of the different dsAAV serotypes in shRNA-mediated HBV suppression

To investigate the relative efficacy of the three dsAAV serotypes in shRNA-based anti-HBV therapy, we selected HBV-S1 shRNA to construct the pseudotyped dsAAV vectors. Our previous study showed that HBV-S1, but not other HBV-specific shRNAs, effectively suppressed HBV replication and gene expression in the ICR/HBV transgenic mouse model.<sup>23</sup> In this study, we used groups of HBV transgenic mice with serum HBV DNA  $> 5 \times 10^7$  genome copies/ml which were IV injected with  $1 \times 10^{12}$  vg per mouse (or  $\sim 3.3 \times 10^{13}$  vg/kg) of dsAAV7, dsAAV8, or dsAAV9 vector expressing HBV-S1 or an irrelevant GL2 shRNA to assess the efficacy of RNAi *in vivo*. **Figure 2a** shows serum HBV titers in each group 2 weeks after dsAAV administration. All the HBV-S1 shRNA-encoding vectors markedly reduced the serum HBV titer (**Figure 2a**). dsAAV8/HBV-S1 had the strongest anti-HBV effect, reducing the serum HBV titer by an average of 2,380-fold. dsAAV7/HBV-S1 and dsAAV9/HBV-S1 were equivalent in HBV suppression, resulting in an average 710- and 800-fold reduction in serum HBV titer, respectively. For all three serotypes, the dsAAV vectors expressing the unrelated GL2 shRNA did not significantly reduce the HBV titer. **Figure 2b** shows the time course of the inhibitory effect of the three different dsAAV/HBV-S1 serotypes. All dsAAV vectors significantly reduced the HBV titer from 1 week after

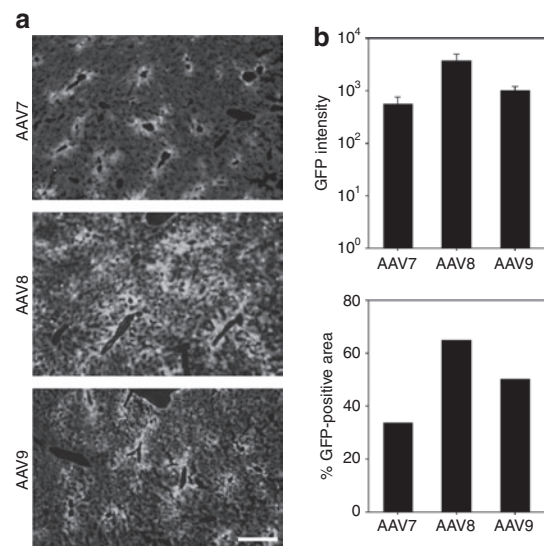


**Figure 1** Comparison of liver transduction efficiency of different double-stranded adeno-associated virus (dsAAV) serotypes. Groups of ICR mice were intravenously injected with  $1 \times 10^{12}$  vector genomes per mouse of dsAAV7/CB-GFP, dsAAV8/CB-GFP, or dsAAV9/CB-GFP vector. **(a)** Photographs of liver cryosections (5  $\mu$ m) were taken 3 weeks after injection and examined for green fluorescent protein (GFP) expression. Original magnification  $\times 40$ . Bar = 500  $\mu$ m. **(b)** Quantification of the average fluorescence intensity and the percentage of the total area containing GFP-positive cells.

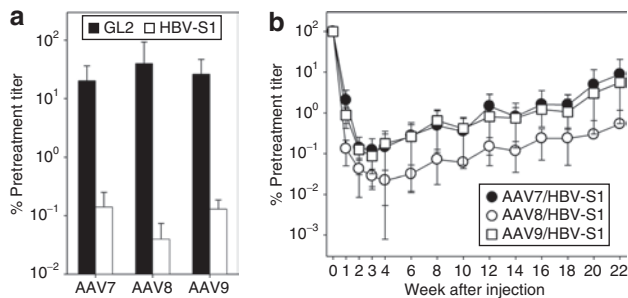


**Figure 2** Comparison of different double-stranded adeno-associated virus (dsAAV) serotypes in small hairpin RNA (shRNA)-mediated hepatitis B virus (HBV) suppression. Groups of HBV transgenic mice ( $n = 4-6$ ) were intravenously injected with  $1 \times 10^{12}$  vector genomes per mouse of dsAAV7, dsAAV8, or dsAAV9 vector expressing control GL2 or HBV-S1 shRNAs. **(a)** Two weeks after injection, serum HBV titers were measured by real-time PCR and are presented as a percentage of the pretreatment titer for the group (mean  $\pm$  SD). **(b)** Time course of HBV suppression after injection of the different dsAAV serotypes encoding HBV-S1 shRNA (mean  $\pm$  SD).

dsAAV treatment, with peak inhibition at weeks 3 and 4, followed by a slow recovery of the HBV titer over the next 4 months. At the end of the observation period (22 weeks after dsAAV administration), significant suppression was still seen in mice treated with all dsAAV serotypes, with dsAAV8/HSV-S1 yielding the best inhibition (190-fold reduction in serum HBV titer compared to the 11- and 18-fold reduction using the dsAAV7/HSV-S1 and dsAAV9/HSV-S1 vectors, respectively).

We then measured levels of liver HBV RNA and DNA in dsAAV/HSV-S1-injected mice by northern and Southern blot analysis of samples obtained 12 weeks after vector injection. Northern blots showed that, consistent with the serum HBV titer results, treatment with dsAAV8/HSV-S1 led to the greatest decrease in HBV mRNA levels (**Figure 3a**). Compared to the saline-treated control, dsAAV8/HSV-S1 resulted in an average 83% reduction in the steady levels of both the 3.5- and 2.4/2.1-kb HBV transcripts when normalized to the expression level of endogenous glyceraldehyde 3-phosphate dehydrogenase mRNA. A significant reduction in HBV mRNA levels was also seen in dsAAV7/HSV-S1- and dsAAV9/HSV-S1-treated mice, but this was lower than in dsAAV8-treated mice, with a respective 53 and 55% reduction in the levels of the 3.5- and 2.4/2.1-kb transcripts for the dsAAV7 vector and a 55 and 64% reduction for the dsAAV9 vector. Southern blot analysis showed that dsAAV-delivered HBV-S1 shRNA had a more pronounced effect on HBV replicative DNA levels than mRNA transcripts. In the dsAAV8/HSV-S1-treated mice, relaxed circular and single-stranded linear viral DNA were virtually undetectable (>97% reduction compared to the saline group). dsAAV7/HSV-S1 and dsAAV9/HSV-S1 also showed a significant reduction in liver HBV DNA levels, with an average 94% reduction for both vectors.

To examine whether the different RNAi efficacies of the three different dsAAV serotypes correlated with their gene transfer efficiency, we performed Southern blot analysis to evaluate the amount of vector DNA in the liver. DNA samples were digested with *HindIII* and *XbaI* to excise an internal fragment

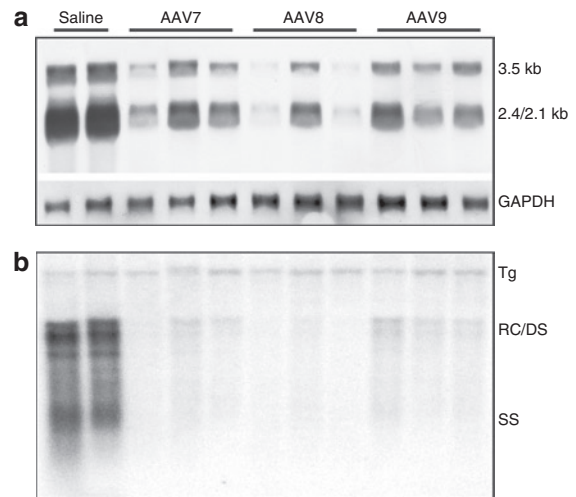


**Figure 3** Reduction in liver hepatitis B virus (HBV) mRNA and DNA levels in transgenic mice by the different double-stranded adeno-associated virus (dsAAV) serotypes. HBV transgenic mice were treated with the different dsAAV serotypes expressing HBV-S1 small hairpin RNA as described in the legend of **Figure 2**, then, 12 weeks after injection, liver samples were collected for northern and Southern blot analysis. **(a)** Northern blot analysis of HBV 3.5-, 2.4-, and 2.1-kb mRNAs, with mouse glyceraldehyde 3-phosphate dehydrogenase (GAPDH) mRNA as the internal control. **(b)** Southern blot analysis of HBV DNA. The bands corresponding to the integrated transgene (Tg) and the HBV replicative DNA intermediates (DS, double-stranded; RC, relaxed circular; SS, single-stranded) are indicated.

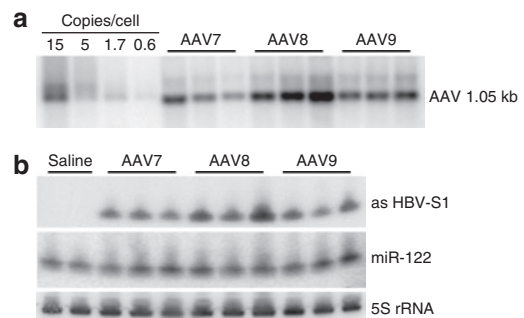


**Figure 4** Copy number of the different double-stranded adeno-associated virus (dsAAV) serotype vectors and small hairpin RNA (shRNA) expression in the liver. Liver samples were obtained from the dsAAV-treated hepatitis B virus (HBV) transgenic mice as described in the legend of **Figure 2**. **(a)** Analysis of dsAAV vector genomes. Total liver DNA (10  $\mu$ g) from mice treated with the different dsAAV serotypes was analyzed by Southern blotting after *Bam*HI and *Xba*I digestion, which releases the 1.05-kb fragment from the AAV genome. The vector plasmid was used as the reference standard for estimation of AAV genome copy number. **(b)** Total liver RNA (30  $\mu$ g) was analyzed by northern blotting using radiolabeled probes specific for the antisense strand of HBV-S1 shRNA ("as HBV-S1") and endogenous microRNA-122.

of 1.05 kb and hybridized with a probe corresponding to the GFP sequence, which present in all the dsAAV vectors. As shown in **Figure 4a**, dsAAV8/HSV-S1-injected mice had the highest amounts of vector DNA in the liver ( $25 \pm 10$  copies per cell). Administration of the same dose of dsAAV7 or dsAAV9 resulted in, respectively, an average of  $7.6 \pm 4$  or  $13 \pm 2$  copies per cell, a reduction of 3.3- or 1.9-fold compared to injection of dsAAV8.

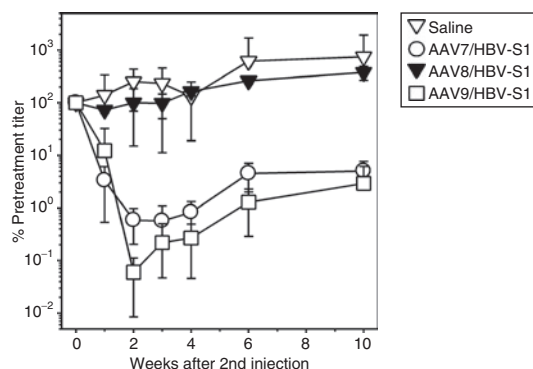


**Figure 5** Preimmunization with double-stranded adeno-associated virus 2/8 (dsAAV2/8) does not block the anti-HBV effect of other dsAAV serotypes expressing HBV-S1 small hairpin RNA (shRNA). Hepatitis B virus (HBV) transgenic mice were initially intravenously injected with  $1 \times 10^{12}$  vector genomes (vg) per mouse of dsAAV2/8/GL2, then, 4 weeks later, were randomly grouped and received a second injection of  $1 \times 10^{12}$  vg per mouse of dsAAV7, dsAAV8, or dsAAV9 vector expressing HBV-S1 shRNA. Mice injected with saline served as controls. Serum HBV titers at the indicated time points after the second injection were determined and are presented as a percentage of the pretreatment titer for the group (mean  $\pm$  SD;  $n = 3$ ).

Next we measured expression levels of the antisense strand of the processed HBV-S1 shRNA in the liver by northern blot analysis using a specific isotope-labeled oligonucleotide probe. Consistent with the result of the AAV vector DNA analysis, mice injected with dsAAV8/HBV-S1 expressed 1.43- or 1.35-fold more HBV-S1 than mice injected with the dsAAV7 or dsAAV9 vector, respectively (Figure 4b, upper panel). A recent report showed that overexpression of shRNAs in mouse liver by dsAAV vectors can lead to hepatotoxicity, which is probably due to competition and interference with endogenous microRNA biogenesis.<sup>28</sup> To determine whether endogenous microRNA expression was affected in our RNAi-treated mice, the membrane was stripped and rehybridized to detect microRNA-122, which is known to be specifically expressed in the liver. We found that endogenous microRNA-122 expression in dsAAV/HBV-S1-treated mice was indistinguishable from that in the saline control animals, or even slightly increased (15–25% increase) (Figure 4b, lower panel). These results clearly show that significant anti-HBV inhibition can be achieved by shRNA-expressing dsAAV vectors without affecting microRNA expression and that the HBV inhibitory effect is mainly determined by the different liver transduction rates of the three dsAAV serotypes.

### HBV suppression by sequential delivery of shRNAs using serologically distinct dsAAV serotypes

To determine whether sequential delivery of shRNAs by the dsAAV7, dsAAV8, and dsAAV9 vectors was possible, we first demonstrated that there was minimal immune cross-reactivity between dsAAV7, dsAAV8, and dsAAV9 by an *in vitro* neutralization assay (Supplementary Figure S1 and Supplementary Materials and Methods). Next, we designed an animal experiment to determine the RNAi effect of the second injection and examine possible cross-reactivity of these dsAAV vectors *in vivo*. HBV transgenic mice were first injected with  $1 \times 10^{12}$  vg per mouse of dsAAV8/GL2, and then were injected 4 weeks later with  $1 \times 10^{12}$  vg per mouse of

dsAAV7/HBV-S1, dsAAV8/HBV-S1, or dsAAV9/HBV-S1. Serum HBV titers were measured to evaluate the RNAi efficacy of the second dsAAV/HBV-S1 injection. As shown in Figure 5, pretreatment with dsAAV8/GL2 completely abrogated the RNAi effect of a subsequent injection of dsAAV8/HBV-S1, serum HBV DNA levels at all time points being comparable to those of the control saline group. In contrast, dsAAV7/HBV-S1 and dsAAV9/HBV-S1 were equally potent at reducing HBV titers in mice previously injected with dsAAV8 vector, the reduction being almost as good as that in naive mice (Figure 2b). These data clearly show that dsAAV7 and dsAAV9 transduction was not affected by the presence of an anti-AAV8 humoral immune response.

Then we investigated whether injection of a second dsAAV vector of a different serotype could prolong RNAi-mediated HBV suppression. Figure 6a and b show results from two independent experiments on, respectively, two and three mice. In both experiments, the initial treatment of the HBV transgenic mice with  $1 \times 10^{12}$  vg per mouse of dsAAV8/HBV-S1 led to a rapid and significant decrease in serum HBV titer, with a maximal reduction of between 260- and 3,570-fold. The RNAi inhibitory effect then gradually diminished, and, by week 56, the titer rose to a level approaching the pretreatment titer in all mice except mouse #1301 (Figure 6b), which still showed an eightfold reduction. In experiment 1, when a second injection of dsAAV9/HBV-S1 at a dose of  $3.3 \times 10^{13}$  vg/kg was given 60 weeks after the initial treatment, up to 10,000-fold reduction in serum HBV titer was seen 3–4 weeks later in both mice (#1318 and #1340) (Figure 6a). In experiment 2, a second injection of the same dose of dsAAV9/HBV-S1 at week 62 led to a 550-, 670-, and 2,500-fold reduction in HBV DNA in mouse #1316, #1301, and #1325, respectively (Figure 6b). Interestingly, we found that the suppressive effect on the HBV titer after the second vector injection decreased much faster than that caused by the first injection. For example, in mouse #1318 in experiment 1, after the second injection, HBV suppression rebounded from >2,000-fold (week 65) to <200-fold (week 69) within 4 weeks, whereas the first dsAAV treatment resulted in >250-fold inhibition for at least 20 weeks in the same mouse.

We designed experiments to investigate the mechanisms leading to the rapid HBV rebound after the second dsAAV RNAi treatment. First, we ruled out the possibility of selection of shRNA-resistant HBV mutants. The genome of HBV isolates ( $N = 3$ ) from the long-term treated animals were sequenced and found that all viruses maintained the wild-type HBV-S1 target sequence. Another possible cause of the rapid HBV rebound might be the presence of AAV-specific T-cell responses, which might be induced by the initial dsAAV8 treatment and boosted by the second dsAAV9 vector. A previous clinical study showed that AAV-induced T cells could cause damage to the transduced hepatocytes, therefore leading to reduced level and duration of transgene expression.<sup>29</sup> To exclude possible immune interference from the previous AAV8 treatment, we designed an experiment by injecting dsAAV9/HBV-S1 in untreated ICR/HBV mice of the same age as those receiving the second injection in the multiple dsAAV treatment experiments described above (Figure 6), and also included 6–8-week-old mice as controls. As shown in Figure 7a, injection of dsAAV9/HBV-S1 resulted in a similar inhibitory effect in the first 4 weeks in both aged and young mice. However, HBV suppression

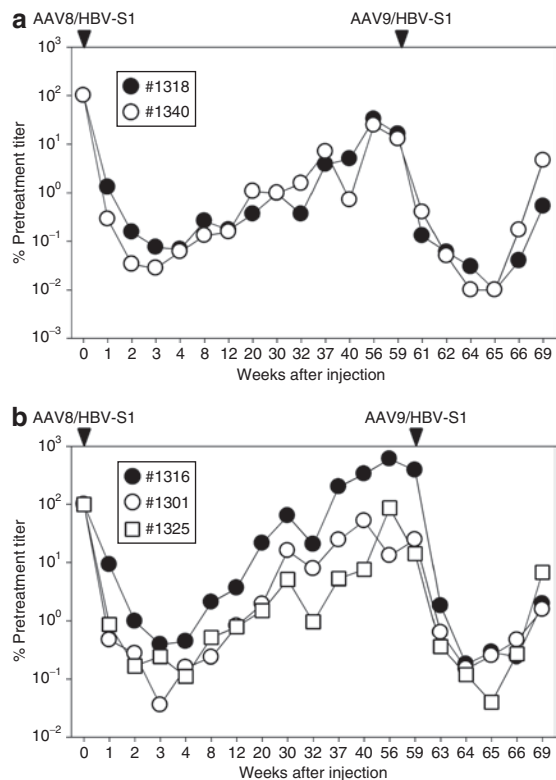


**Figure 6** Effect of multiple administration of double-stranded adeno-associated virus (dsAAV) vectors expressing HBV-S1 small hairpin RNA in transgenic mice. (a,b) The data for two independent experiments on (a) two mice or (b) three mice. Hepatitis B virus (HBV) transgenic mice (6–8-weeks old) were injected with  $1 \times 10^{12}$  vector genomes (vg) per mouse of dsAAV2/8/HSV-S1, then, (a) 60 or (b) 62 weeks later, were re-injected with dsAAV2/9/HSV-S1 at a dose of  $3.3 \times 10^{13}$  vg/kg. Serum HBV titers at the indicated time points were measured and are presented as a percentage of the pretreatment titer for the same mouse.

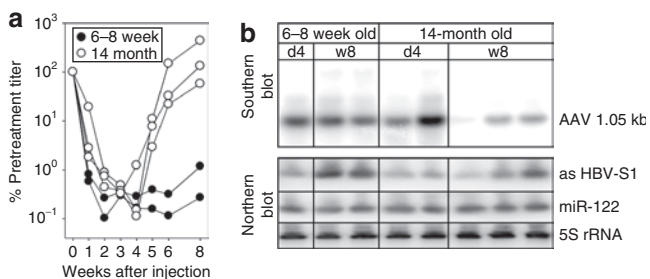


**Figure 7** Hepatitis B virus (HBV) suppression by double-stranded adeno-associated virus 9 (dsAAV9)/HBV-S1 in young and aged transgenic mice. HBV transgenic mice at the age of 6–8-week or 14-month old were injected with  $3.3 \times 10^{13}$  vg/kg of dsAAV9/HSV-S1. (a) Serum HBV titers at the indicated time points after injection were measured and presented as described in the legend of **Figure 2**. (b) Total liver DNA and RNA were collected at the indicated time points. Southern and northern blots were used to analyze the amount of AAV DNA (upper panel) and antisense HBV-S1 shRNA, miR-122, and 5S rRNA (lower panel), respectively.

in the aged mice rapidly decreased from week 5 and by week 8 HBV titers in all mice of this group returned to the pretreatment level (**Figure 7a**). By contrast, the RNAi silencing effect in young HBV transgenic mice persisted stably within the 8-week observation period (**Figure 7a**). Southern blot analysis showed that the

amount of AAV vector DNA in the liver of aged mice decreased by an average of 6.5-fold within 8 weeks, but remained relatively stable in the young mice (**Figure 7b**, upper panel). Accordingly, the antisense strand of HBV-S1 shRNA also decreased much more rapidly in the aged mice than that in the young mice (**Figure 7b**, lower panel). Expression levels of the control miR-122 and 5S rRNA remained stable in both young and aged mice. Together, these results suggest that the rapid loss of RNAi effects after the secondary dsAAV injection was independent of dsAAV8 pretreatment; instead, this phenomenon is closely related to the age of the treated animals.

## DISCUSSION

The main goal of this study was to develop and improve novel RNAi-based gene therapies for the treatment of chronic HBV infection, which responds poorly to current antiviral regimens.<sup>6,30</sup> We used ICR/HBV transgenic mice as a model system in which the majority of hepatocytes constitutively produce large amount of HBV proteins and viral particles, which thus represent a more clinically relevant and challenging target for antiviral treatment. Our previous study showed that the shRNA-expressing dsAAV8 vector had a marked anti-HBV effect in these transgenic mice.<sup>23</sup> However, the effect weakened with time, which might probably in part due to a gradual decline in AAV copy number in the transduced hepatocytes. Multiple administrations of serologically non-cross-reactive AAV serotypes represent an attractive approach to prolong the RNAi-mediated anti-HBV effect. In this report, we compared the three hepatotropic dsAAV vectors, dsAAV7, dsAAV8, and dsAAV9, for their *in vivo* transduction efficiency and ability to suppress HBV replication and gene expression in the transgenic mouse model. Our results showed that all three vectors infected a significant number of hepatocytes and caused profound suppression of serum and liver HBV, with dsAAV8 vector having the greatest inhibitory effect. More importantly, we showed that a significant anti-HBV effect could be achieved by readministration of a serologically distinct dsAAV vector carrying the same shRNA. Thus, by combining the power of the RNAi silencing effect and the strategy of multiple dsAAV injections, a maximum anti-HBV effect could be achieved and maintained, which might provide great benefit for chronic HBV patients.

Of the three hepatotropic dsAAV vectors tested, dsAAV8 consistently had the best RNAi-mediated anti-HBV effect at all time points analyzed. For example, at 2 weeks after dsAAV administration (**Figure 2a**), dsAAV8/HSV-S1 reduced the serum HBV titer by an average of 2,380-fold compared to the average 710- and 800-fold reduction by dsAAV7/HSV-S1 and dsAAV9/HSV-S1, respectively. dsAAV8/HSV-S1 also caused the largest decrease in liver HBV RNA and DNA levels (**Figure 3a** and **b**). The superior anti-HBV effect of the dsAAV8 vector was because of its higher liver transduction efficiency of 65% compared to the values of 34 or 50% for the dsAAV7 or dsAAV9 vector, respectively (**Figure 1a**), which might be ascribed to the rapid uncoating of the AAV8 capsid after entry into hepatocytes.<sup>31,32</sup> These characteristics allowed the dsAAV8 vector to deliver the highest amounts of AAV genome in the liver (an average of 25 copies per cell versus 7.6 and 13 copies per cell for dsAAV7 and dsAAV9, respectively) (**Figure 4a**) and, consequently, produced more antisense strand of

HBV-S1 shRNA (1.43- and 1.35-fold higher than that produced by dsAAV7 and dsAAV9, respectively) (Figure 4b). Interestingly, the dsAAV7 vector was as effective as dsAAV9 in inhibiting HBV replication and gene expression (Figures 2 and 3), but the liver transduction rate for dsAAV7 (34%) was significantly lower than that achieved using dsAAV9 (50%) (Figure 1). One major difference between dsAAV7 and dsAAV9 in liver transduction was that dsAAV7 transduction was essentially restricted to the centrilobular hepatocytes (Figure 1a), whereas dsAAV9 transduction was relatively uniform throughout the liver section. The preferential gene delivery to the centrilobular hepatocytes by the dsAAV7 vector might help increase its overall anti-HBV effect, because HBV replication is mainly restricted to the cytoplasm of these centrilobular hepatocytes in the transgenic mouse model.<sup>23,33</sup>

In this study (Figure 2) and in our previous report,<sup>23</sup> we showed that a single treatment with dsAAV vectors expressing HBV-S1 shRNA dramatically decreased serum and liver HBV within 1 month, but the RNAi effect gradually decreased with time. This result conflicts with those in other reports, which showed that, regardless of vector genome structure (single-stranded or double-stranded), AAV vectors, particularly the AAV8 serotype, are able to produce and sustain high levels of transgene expression in the liver for months to years in various animal models.<sup>26,34,35</sup> The decline in the RNAi effect in our studies was, at least in part, due to the decrease in AAV genome copy number in the liver.<sup>23</sup> It is known from studies employing partial hepatectomy that the majority of the injected AAV vector in hepatocytes remains episomal (>90%), rather than becoming integrated into the hepatocyte chromosome.<sup>36</sup> Thus, the amount of AAV DNA, as well as the level of transgene expression, decreases more rapidly during liver growth or hepatocyte regeneration.<sup>37,38</sup> Our unpublished results and the results of several other studies<sup>2,39,40</sup> show that mice carrying partial or complete HBV genomes are prone to spontaneous or exogenous hepatic damage because of the accumulation of high levels of HBV proteins and viral particles. The enhanced hepatocyte damage in HBV transgenic mice would theoretically induce regenerative stimuli and subsequently compensatory liver proliferation. Thus, the more rapid decrease in AAV DNA in HBV transgenic mice might be partially due to a higher liver turnover rate in this animal model.

Multiple AAV administration represents an attractive approach to prolonging the RNAi-mediated anti-HBV effect in the HBV transgenic mouse model. Host humoral immune responses directed against the AAV capsid protein induced by previous injections might prevent subsequent treatment with AAV vectors with the same capsid.<sup>41,42</sup> To overcome this problem, several groups have demonstrated that efficient gene delivery can be achieved in the presence of preexisting immunity using non-cross-reactive AAV serotypes.<sup>26,27,43</sup> In this study, we used animal experiments to examine whether the RNAi effect could be induced by a second injection with a different dsAAV vector. In an *in vivo* cross-administration experiment, we showed that anti-AAV8 immunity completely blocked the dsAAV8/HBV-S1-mediated anti-HBV activity, but did not interfere with the effect of dsAAV7/HBV-S1 or dsAAV9/HBV-S1 (Figure 5). Most importantly, we showed that injection of dsAAV9/HBV-S1 into dsAAV8/HBV-S1-pretreated transgenic mice at a time when the HBV titer had returned to the

pretreatment level resulted in a similar decrease in serum HBV DNA to that seen in naive mice treated with the same dsAAV9 vector (Figure 6). These results provide evidence that the sequential use of different dsAAV serotypes can prolong the RNAi-mediated HBV suppression. The three hepatotropic AAV vectors are highly homologous in capsid amino acid composition (88% homology between AAV8 and AAV7 and 85% between AAV8 and AAV9).<sup>19,24</sup> The lack of cross-reactivity between these AAV vectors is probably due to the presence of several variable regions in the capsid protein that are responsible for receptor binding and antibody recognition.<sup>44</sup> Multiple administration of different dsAAV serotypes carrying a different shRNA also provides a means against RNAi-selected mutant viruses, which escape the original RNAi inhibition by mutating the target sequence after prolonged treatment.<sup>13,45,46</sup>

Interestingly, in the multiple dsAAV treatment study we found that the suppressive effect of RNAi after the second dsAAV injection decreased much faster than that caused by the first injection (Figure 6a and b). The quick HBV rebound was not due to selection of RNAi-resistant HBV mutants, because sequencing HBV isolates from the long-term treated animals revealed no mutation in the HBV-S1 target sequence. The unstable RNAi effect after the second injection was neither related to the previous dsAAV treatment. This is proved by treating naive HBV mice, which never encountered dsAAV before, with the same amount of dsAAV9, and showed that by 8 week after injection HBV quickly rebound to the pretreatment level in the aged but not the young mice (Figure 7a). These results suggest the rapid loss of RNAi effects was closely related to the age of the mice when receiving dsAAV treatment. The AAV dilution effect caused by hepatocyte regeneration as discussed above might also explain the unstable RNAi effects observed in the aged mice, which presumably experience higher levels of liver damage and enhanced proliferation than younger mice (Figures 6 and 7). Interestingly, after dsAAV9/HBV-S1 injection we observed an even faster HBV rebound in the aged but previously untreated mice than in mice that received RNAi treatment in the young age. In the latter group, the long-term HBV suppression by the first RNAi therapy presumably could alleviate liver damage in the transgenic mice, and thus these animals might have slower hepatocyte regeneration rate than those in the former group. We are currently investigating the hepatocyte turnover rate in RNAi-treated and untreated HBV transgenic mice to further clarify this issue.

A recent report by Grimm *et al.*<sup>28</sup> showed that effective anti-HBV RNAi therapy using a similar self-complementary AAV8 vector was associated with dose-dependent liver injury and even animal death. This toxic effect was probably due to overexpression of shRNA, which might interfere with endogenous microRNA processing and functionality. However, in our study, none of the animals receiving long-term RNAi therapy showed liver damage (normal alanine aminotransferase levels, data not shown) or mortality, even the AAV dosage being increased to  $3 \times 10^{12}$  vg per mouse (data not shown), three times higher than the reported toxic doses in Grimm's study. Furthermore, analysis of microRNA expression in our dsAAV-treated mice showed that levels of endogenous microRNA-122 in the liver were not different from those in the control animals (Figure 4b, lower panel). One of the

main differences between the study of Grimm *et al.* and our own is promoter usage, as the H1 promoter was used in our system and the U6 promoter in Grimm's study. The U6 promoter-driven shRNA has been reported to cause cell death by apoptosis, and toxicity was prevented by replacing the U6 promoter with the H1 promoter.<sup>47</sup> We are currently investigating whether the U6 promoter is the major cause of toxicity by replacing the H1 promoter in our AAV vector with the U6 promoter.

In summary, our study underscores the potential of the multiple administrations of different dsAAV serotypes in inducing persistent RNAi suppression. Long-term HBV suppression can be achieved in the absence of any obvious RNAi- or vector-associated toxicity. We believe this approach could be further developed to become a convenient and effective treatment for keeping the HBV titer below a certain threshold, which might be beneficial in protecting chronic HBV patients from developing progressive liver diseases.

## MATERIALS AND METHODS

**dsAAV vector preparation.** Plasmids pAAVEMBL-CMV-GFP and pAAVEMBL-CB-GFP containing the *GFP* transgene driven, respectively, by the cytomegalovirus (CMV) promoter or the chicken  $\beta$ -actin promoter have been described elsewhere.<sup>48</sup> These plasmids were designed to produce dsAAV genomes by introducing a deletion of the D-sequence and terminal resolution site into one end of the AAV2 inverted terminal repeat.<sup>48</sup> Construction of pAAVEMBL/HBV-S1 and pAAVEMBL/GL2, which encode, respectively, a HBV- or a firefly luciferase-specific shRNA transcript under the control of the H1 promoter, has been described previously.<sup>23</sup> The CMV promoter of the original pAAVEMBL-CMV-GFP plasmid was deleted, but the GFP coding sequence was preserved to maintain the size of the dsAAV genome at ~1.5 kb for dsAAV packaging. The pseudotyped dsAAV7, dsAAV8, and dsAAV9 vectors were generated by cross-packaging the pAAVEMBL plasmid with plasmids containing each individual serotype-specific capsid gene as described previously.<sup>37</sup> The recombinant dsAAV vectors were purified by two rounds of CsCl sedimentation. The physical vector titers were assessed by quantitative PCR amplification of DNase-protected particles using SYBR Green reaction mix (Roche Diagnostics, Mannheim, Germany) and primers (sense: 5'-ACGTCTATATCATGGCCG-3'; antisense: 5'-TGTGATCGCGTTCTC-3') specific for the common *GFP* sequence presenting in all pAAVEMBL plasmids.

**Animals and vector administration.** Wild-type ICR mice (purchased from BioLASCO, Ilan, Taiwan) and HBV transgenic mice (line Tg[HBV1.3]24-3), which contain a 1.3-times overlength HBV genome of the ayw subtype on the ICR background,<sup>23</sup> were used. This HBV transgenic mouse line produces high levels of HBV replicative DNA and all forms of viral mRNAs and proteins in the liver, which mimics the situation in progressive chronic HBV-infected patients. To measure the liver transduction rate, wild-type ICR mice were IV injected with  $1 \times 10^{12}$  vg per mouse (or  $\sim 3.3 \times 10^{13}$  vg/kg) of different dsAAV serotype vectors expressing GFP driven by the CB promoter, then, 3 weeks later, liver fragments were isolated for GFP analysis. To evaluate the RNAi-mediated anti-HBV effect, 6–8-week- or 14-month-old male HBV transgenic mice with serum HBV titers of  $> 5 \times 10^7$  genome copies/ml were IV injected with  $1 \times 10^{12}$  vg per mouse (young mice) or  $3.3 \times 10^{13}$  vg/kg (aged mice) of different dsAAV serotype vectors encoding HBV-S1 or GL2 shRNAs, and serum and liver samples were collected at different times for analysis. For cross-administration experiments, HBV transgenic mice were IV injected with  $1 \times 10^{12}$  vg of dsAAV8/GL2, then, 4 weeks later, with  $1 \times 10^{12}$  vg per mouse of dsAAV7/HBV-S1, dsAAV8/HBV-S1, or dsAAV9/HBV-S1. To investigate the RNAi effect of multiple AAV injections, HBV transgenic mice were IV injected

with  $1 \times 10^{12}$  vg per mouse of dsAAV8/HBV-S1, then with dsAAV9/HBV-S1 60–62 weeks later. The amount of dsAAV vector used in the second injection was increased to keep the final dsAAV dose at  $3.3 \times 10^{13}$  vg/kg. All animals were housed in a specific pathogen-free environment in the animal facility of the Institute of Biomedical Sciences, Academia Sinica. All experimental procedures were in compliance with Academia Sinica IACUS and Council of Agriculture Guidebook for the Care and Use of Laboratory Animals.

**Detection of GFP expression.** To detect GFP expression, liver fragments were embedded in optimal cutting temperature medium and cryosections (5  $\mu$ m) were mounted on positively charged slides and examined by fluorescence microscopy. For quantitative analysis of GFP intensity, at least 5 observation fields per section were randomly photographed with constant exposure conditions to keep the data comparable. The average intensity and the GFP-positive area were analyzed using Image-Pro Plus software (version 6.2; Media Cybernetics, Atlanta, GA). The percentage of the total area containing GFP-positive cells was calculated as (GFP-positive area/total liver area)  $\times$  100%.

**Analysis of HBV DNA and RNA.** Serum samples were collected at different time points and DNA were extracted to measure the HBV viral load. A sensitive hybridization probe-based real-time PCR was used to measure the HBV titer. The sequences of the primers were: forward primer (HBV1.3fw), 5'-CTCCACCAATCGCCAGTC-3'; reverse primer (HBV1.3as); 5'-ATCCTCGAGAAGATTGACGATAAT-3'; 3'-fluorescein (fam)-labeled donor probe, 5'-CATGGCCTGAGGATGAGTGTCTTCTCA-3'; and 5'-Red640-labeled acceptor probe, 5'-AGGTGGAGACAGCGGGGTAGG-3' (LightCycler FastStart; Roche Diagnostics). Plasmid pHBV1.3 of tenfold dilutions ( $1.33 \times 10^3$  to  $1.33 \times 10^9$  copies/ml) was used to generate a standard curve in parallel PCRs. The liver fragments were mechanically ground in liquid nitrogen and resuspended in lysis buffer (100 mmol/l NaCl, 10 mmol/l Tris, pH 7.4, 1 mmol/l EDTA, 0.5% sodium dodecyl sulfate, supplemented with 100  $\mu$ g/ml of proteinase K and 100  $\mu$ g/ml RNaseA) at 37°C for 12–16 hours to digest tissues. Total DNA were extracted using phenol/chloroform and analyzed by Southern blot analysis of 10  $\mu$ g of DNA digested with *Hind*III, which does not cut within the HBV transgene. The samples were separated on an agarose gel, transferred to a nylon membrane (Amersham Biosciences, Piscataway, NJ), and hybridized with a <sup>32</sup>P-labeled HBV-specific DNA probe (Rediprime II, GE Healthcare, Piscataway, NJ). Signals were developed using phosphor screens and analyzed using ImageQuant software (Molecular Dynamics, Sunnyvale, CA). Total RNA was isolated using TRIZOL reagent according to the manufacturer's instructions (Invitrogen, Carlsbad, CA). For northern blot analysis, 10  $\mu$ g of total liver RNA was separated by electrophoresis on a 1% agarose formaldehyde gel and transferred to a nylon membrane, then the blot was hybridized with a biotin-labeled HBV or glyceraldehyde 3-phosphate dehydrogenase probe which were prepared with North2South Biotin Random Prime DNA Labeling Kit (Pierce, Rockford, IL). Signals were visualized by chemiluminescence (Pierce) and analyzed using ImageQuant software.

**Detection of AAV DNA.** To detect AAV DNA in the liver, 10  $\mu$ g of total liver DNA, digested with *Hind*III and *Xba*I to release a 1.05-kb fragment, was subjected to Southern blot analysis. The blot was probed with a <sup>32</sup>P-labeled DNA fragment corresponding to the *GFP* coding sequence, which is present in all pAAVEMBL vectors used in this study. Amounts of the pAAVEMBL plasmid corresponding to 0.6–15 copies per diploid genome were used as standards. Southern blot hybridization and quantification of signals were performed as described in the earlier section.

**Small RNA northern blot analysis.** For small RNA northern blot analysis, 30  $\mu$ g of total liver RNA from dsAAV-treated animals was separated on a 15% polyacrylamide-urea gel, transferred to a nylon membrane, and hybridized to <sup>32</sup>P-labeled oligonucleotides (19 nt) corresponding to the antisense strand of the HBV-S1 shRNA, microRNA-122, or 5S rRNA. Equal

RNA loading was assessed by ethidium bromide staining. ImageQuant software was used to quantify small RNA signals as described above.

## SUPPLEMENTARY MATERIAL

**Figure S1.** Serologic cross-reactivity of the different dsAAV serotypes.

**Materials and Methods.** Anti-AAV neutralization assay.

## ACKNOWLEDGMENTS

This work is supported by Grant NSC96-2320-B-001 from National Science Council (Taipei, Taiwan). None of the authors declares a financial conflict of interest.

## REFERENCES

- Ganem, D and Prince, AM (2004). Hepatitis B virus infection—natural history and clinical consequences. *N Engl J Med* **350**: 1118–1129.
- Kremsdorf, D, Soussan, P, Paterlini-Brechot, P and Brechot, C (2006). Hepatitis B virus-related hepatocellular carcinoma: paradigms for viral-related human carcinogenesis. *Oncogene* **25**: 3823–3833.
- Chen, CJ, Yang, HI, Su, J, Jen, CL, You, SL, Lu, SN *et al.* (2006). Risk of hepatocellular carcinoma across a biological gradient of serum hepatitis B virus DNA level. *JAMA* **295**: 65–73.
- Yang, HI, Lu, SN, Liaw, YF, You, SL, Sun, CA, Wang, LY *et al.* (2002). Hepatitis B e antigen and the risk of hepatocellular carcinoma. *N Engl J Med* **347**: 168–174.
- Langley, DR, Walsh, AW, Baldick, CJ, Eggers, BJ, Rose, RE, Levine, SM *et al.* (2007). Inhibition of hepatitis B virus polymerase by entecavir. *J Virol* **81**: 3992–4001.
- Mailliard, ME and Gollan, JL (2006). Emerging therapeutics for chronic hepatitis B. *Annu Rev Med* **57**: 155–166.
- Dykhhoorn, DM and Lieberman, J (2006). Running interference: prospects and obstacles to using small interfering RNAs as small molecule drugs. *Annu Rev Biomed Eng* **8**: 377–402.
- Grimm, D and Kay, MA (2006). Therapeutic short hairpin RNA expression in the liver: viral targets and vectors. *Gene Ther* **13**: 563–575.
- Arbuthnot, P, Longshaw, V, Naidoo, T and Weinberg, MS (2007). Opportunities for treating chronic hepatitis B and C virus infection using RNA interference. *J Viral Hepat* **14**: 447–459.
- Konishi, M, Wu, CH and Wu, GY (2003). Inhibition of HBV replication by siRNA in a stable HBV-producing cell line. *Hepatology* **38**: 842–850.
- McCaffrey, AP, Nakai, H, Pandey, K, Huang, Z, Salazar, FH, Xu, H *et al.* (2003). Inhibition of hepatitis B virus in mice by RNA interference. *Nat Biotechnol* **21**: 639–644.
- Shlomai, A and Shaul, Y (2003). Inhibition of hepatitis B virus expression and replication by RNA interference. *Hepatology* **37**: 764–770.
- Wu, HL, Huang, LR, Huang, CC, Lai, HL, Liu, CJ, Huang, YT *et al.* (2005). RNA interference-mediated control of hepatitis B virus and emergence of resistant mutant. *Gastroenterology* **128**: 708–716.
- Giladi, H, Ketzinil-Gilad, M, Rivkin, L, Felig, Y, Nussbaum, O and Galun, E (2003). Small interfering RNA inhibits hepatitis B virus replication in mice. *Mol Ther* **8**: 769–776.
- Morrissey, DV, Blanchard, K, Shaw, L, Jensen, K, Lockridge, JA, Dickinson, B *et al.* (2005). Activity of stabilized short interfering RNA in a mouse model of hepatitis B virus replication. *Hepatology* **41**: 1349–1356.
- Morrissey, DV, Lockridge, JA, Shaw, L, Blanchard, K, Jensen, K, Breen, W *et al.* (2005). Potent and persistent *in vivo* anti-HBV activity of chemically modified siRNAs. *Nat Biotechnol* **23**: 1002–1007.
- Grieger, JC and Samulski, RJ (2005). Adeno-associated virus as a gene therapy vector: vector development, production and clinical applications. *Adv Biochem Eng Biotechnol* **99**: 119–145.
- Warrington, KH Jr and Herzog, RW (2006). Treatment of human disease by adeno-associated viral gene transfer. *Hum Genet* **119**: 571–603.
- Gao, GP, Alvira, MR, Wang, L, Calcedo, R, Johnston, J and Wilson, JM (2002). Novel adeno-associated viruses from rhesus monkeys as vectors for human gene therapy. *Proc Natl Acad Sci USA* **99**: 11854–11859.
- Davidoff, AM, Gray, JT, Ng, CY, Zhang, Y, Zhou, J, Spence, Y *et al.* (2005). Comparison of the ability of adeno-associated viral vectors pseudotyped with serotype 2, 5, and 8 capsid proteins to mediate efficient transduction of the liver in murine and nonhuman primate models. *Mol Ther* **11**: 875–888.
- Nakai, H, Fuess, S, Storm, TA, Muramatsu, S, Nara, Y and Kay, MA (2005). Unrestricted hepatocyte transduction with adeno-associated virus serotype 8 vectors in mice. *J Virol* **79**: 214–224.
- Nathwani, AC, Gray, JT, Ng, CY, Zhou, J, Spence, Y, Waddington, SN *et al.* (2006). Self-complementary adeno-associated virus vectors containing a novel liver-specific human factor IX expression cassette enable highly efficient transduction of murine and nonhuman primate liver. *Blood* **107**: 2653–2661.
- Chen, CC, Ko, TM, Ma, HI, Wu, HL, Xiao, X, Li, J *et al.* (2007). Long-term inhibition of hepatitis B virus in transgenic mice by double-stranded adeno-associated virus 8-delivered short hairpin RNA. *Gene Ther* **14**: 11–19.
- Gao, G, Vandenberghe, LH, Alvira, MR, Lu, Y, Calcedo, R, Zhou, X *et al.* (2004). Clades of adeno-associated viruses are widely disseminated in human tissues. *J Virol* **78**: 6381–6388.
- Hildinger, M, Auricchio, A, Gao, G, Wang, L, Chirmule, N and Wilson, JM (2001). Hybrid vectors based on adeno-associated virus serotypes 2 and 5 for muscle-directed gene transfer. *J Virol* **75**: 6199–6203.
- Wang, L, Calcedo, R, Nichols, TC, Bellinger, DA, Dillow, A, Verma, IM *et al.* (2005). Sustained correction of disease in naive and AAV2-pretreated hemophilia B dogs: AAV2/8-mediated, liver-directed gene therapy. *Blood* **105**: 3079–3086.
- Riviere, C, Danos, O and Douar, AM (2006). Long-term expression and repeated administration of AAV type 1, 2 and 5 vectors in skeletal muscle of immunocompetent adult mice. *Gene Ther* **13**: 1300–1308.
- Grimm, D, Streetz, KL, Jopling, CL, Storm, TA, Pandey, K, Davis, CR *et al.* (2006). Fatality in mice due to oversaturation of cellular microRNA/short hairpin RNA pathways. *Nature* **441**: 537–541.
- Manno, CS, Arruda, VR, Pierce, GF, Glader, B, Ragni, M, Rasko, J *et al.* (2006). Successful transduction of liver in hemophilia by AAV-Factor IX and limitations imposed by the host immune response. *Nat Med* **12**: 342–347.
- Férris, G, Kaptein, S, Neyts, J and De Clercq, E (2007). Antiviral treatment of chronic hepatitis B virus infections: the past, the present and the future. *Rev Med Virol* **18**: 19–34.
- Wang, J, Xie, J, Lu, H, Chen, L, Hauck, B, Samulski, RJ *et al.* (2007). Existence of transient functional double-stranded DNA intermediates during recombinant AAV transduction. *Proc Natl Acad Sci USA* **104**: 13104–13109.
- Thomas, CE, Storm, TA, Huang, Z and Kay, MA (2004). Rapid uncoating of vector genomes is the key to efficient liver transduction with pseudotyped adeno-associated virus vectors. *J Virol* **78**: 3110–3122.
- Guidotti, LG, Matzke, B, Schaller, H and Chisari, FV (1995). High-level hepatitis B virus replication in transgenic mice. *J Virol* **69**: 6158–6169.
- Gao, GP, Lu, Y, Sun, X, Johnston, J, Calcedo, R, Grant, R *et al.* (2006). High-level transgene expression in nonhuman primate liver with novel adeno-associated virus serotypes containing self-complementary genomes. *J Virol* **80**: 6192–6194.
- Sarkar, R, Tetreault, R, Gao, G, Wang, L, Bell, P, Chandler, R *et al.* (2004). Total correction of hemophilia A mice with canine FVIII using an AAV 8 serotype. *Blood* **103**: 1253–1260.
- Nakai, H, Yant, SR, Storm, TA, Fuess, S, Meuse, L and Kay, MA (2001). Extrachromosomal recombinant adeno-associated virus vector genomes are primarily responsible for stable liver transduction *in vivo*. *J Virol* **75**: 6969–6976.
- Wang, Z, Zhu, T, Qiao, C, Zhou, L, Wang, B, Zhang, J *et al.* (2005). Adeno-associated virus serotype 8 efficiently delivers genes to muscle and heart. *Nat Biotechnol* **23**: 321–328.
- Bostick, B, Ghosh, A, Yue, Y, Long, C and Duan, D (2007). Systemic AAV-9 transduction in mice is influenced by animal age but not by the route of administration. *Gene Ther* **14**: 1605–1609.
- Zheng, Y, Chen, WL, Louie, SG, Yen, TS and Ou, JH (2007). Hepatitis B virus promotes hepatocarcinogenesis in transgenic mice. *Hepatology* **45**: 16–21.
- Huang, SN and Chisari, FV (1995). Strong, sustained hepatocellular proliferation precedes hepatocarcinogenesis in hepatitis B surface antigen transgenic mice. *Hepatology* **21**: 620–626.
- Halbert, CL, Standaert, TA, Wilson, CB and Miller, AD (1998). Successful readministration of adeno-associated virus vectors to the mouse lung requires transient immunosuppression during the initial exposure. *J Virol* **72**: 9795–9805.
- Manning, WC, Zhou, S, Bland, MP, Escobedo, JA and Dwarki, V (1998). Transient immunosuppression allows transgene expression following readministration of adeno-associated viral vectors. *Hum Gene Ther* **9**: 477–485.
- Halbert, CL, Rutledge, EA, Allen, JM, Russell, DW and Miller, AD (2000). Repeat transduction in the mouse lung by using adeno-associated virus vectors with different serotypes. *J Virol* **74**: 1524–1532.
- Nam, HJ, Lane, MD, Padron, E, Gurda, B, McKenna, R, Kohlbrenner, E *et al.* (2007). Structure of adeno-associated virus serotype 8, a gene therapy vector. *J Virol* **81**: 12260–12271.
- Gitlin, L, Karelsky, S and Andino, R (2002). Short interfering RNA confers intracellular antiviral immunity in human cells. *Nature* **418**: 430–434.
- Das, AT, Brummelkamp, TR, Westerhout, EM, Vink, M, Madiredjo, M, Bernards, R *et al.* (2004). Human immunodeficiency virus type 1 escapes from RNA interference-mediated inhibition. *J Virol* **78**: 2601–2605.
- An, DS, Qin, FX, Auyeung, VC, Mao, SH, Kung, SK, Baltimore, D *et al.* (2006). Optimization and functional effects of stable short hairpin RNA expression in primary human lymphocytes via lentiviral vectors. *Mol Ther* **14**: 494–504.
- Wang, Z, Ma, HI, Li, J, Sun, L, Zhang, J and Xiao, X (2003). Rapid and highly efficient transduction by double-stranded adeno-associated virus vectors *in vitro* and *in vivo*. *Gene Ther* **10**: 2105–2111.